AAS 17-401

OPTICAL SENSOR FOLLOW-UP TASKING ON HIGH PRIORITY UNCORRELATED TRACK

Timothy S. Murphy*, Marcus J. Holzinger†, K. Kim Luu‡, Chris Sabol‡,

This work proposes a methodology for tasking of electro-optical sensors to search an area of state space for a particular object. This work enables current space situational awareness programs to more efficiently follow-up on an unknown object. In particular, this work looks at searching for an unknown space object with prior knowledge in the form of a set, which can be defined via an uncorrelated track. The follow-up can occur from a different location at a different time, which often requires searching a large region of the sky. This work analyzes the divergence of a search region to inform a time optimal search method. Simulation work is included to explore the effects of sensor geometry, initial detection uncertainty, and handoff delay time on total time and feasibility of follow-up.

INTRODUCTION

Background

The space domain awareness (SDA) mission continues to require increased efficiency for catalog upkeep and catalog expansion [2]. As the Space Surveillance Network expands, increased numbers of sensors will become available, allowing for more complex operations. Additional pushes have been made to look for alternative data collection via either dedicated space based sensors or unconventional optical sensors in space such as star trackers [1]. This work in particular will focus on the electro-optical sensor (EOS), that is, cameras. In many cases, these sensors will make large numbers of detections on space objects (SO), some of which may appear with a unique trajectory and photometric signature that warrants follow-up. As of now, there is limited work on how to act on this information without collocated sensors.

A variety of sensor tasking strategies have been proposed, which typically look at the tasking problem in terms of catalog upkeep [5, 14, 10]. These techniques tend to look at the strategic tasking problem, that is, how to use a network of sensor to look at a catelog of objects. This work looks at the tactical tasking problem, that is, given an object and a sensor, how should the sensor look for the object? In particular, this work builds off a particle based search strategy proposed by Hobson [9]. Long term, this work will be combined with modern models for prior information in space objects, namely sequential Bayesian filters [4, 3].

This paper will look at how to search through a set of orbits. In particular, an uncorrelated track (UCT), obtained from an EOS, can be used to define an admissible region [12, 16]. This set of

*Graduate Student, The Guggenheim School of Aerospace Engineering, Georgia Institute of Technology, Georgia Institute of Technology North Ave NW, Atlanta, GA 30332.

†Assistant Professor, The Guggenheim School of Aerospace Engineering, Georgia Institute of Technology, Georgia Institute of Technology North Ave NW, Atlanta, GA 30332. AIAA Senior Member

‡Air Force Research Lab, Kihei, HI, 96753

orbits can be propagated and projected into the field of regard of new sensors. In general, this region can be much larger than the field of view of a sensor, and requires multiple observations [7]. Existing methods are based on a greedy maximum probability observation technique, which looks at observing the densest region of probability [8]. The biggest problems facing this technique are how to choose an optimal trajectory, and what type of optimality is desirable. This paper argues that time optimality is the highest priority. Many SDA sensor systems have a problem of too many objects and not enough sensors, making time on high sensitivity sensors a priority. When searching a set of orbits, there typically is no maximum probability observation that makes sense. Furthermore, when searching a PDF, a greedy maximum probability observation may take significantly more time if an object appears on the fringes of the PDF. Finally, an EOS can be prone to false detections; it is typically more wise to search the entire follow up space than to trust the first detection that is made.

This optimization problem is the covering salesman problem (CSP), a variation of the traveling salesman problem [6]. The CSP looks for the optimal path to take between a series of points such that every point, or a point within a limiting distance, is visited. The tasking problem outlined above has a further complication over the classic CSP, in that the points to be visited have dynamics, and typically spread out as time passes. This problem will in general be NP-hard, and obtaining optimal solutions is difficult. This paper will therefore both attempt the time optimal optimization, but also develop tools that can efficiently analyze the search. Once an observation is made, there exist a variety of techniques for making correlation [18]. This problem is also relevant to allowing non-collocated EOS to observe a single object simultaneously for fast orbit determination [13]. This work looks at the feasibility of different handoff techniques.

Broad Categories of Search

This paper acknowledges two categories in which the search described in this paper would be useful. The first is the problem of how to search an area of state space in order to maintain custody of objects in it. In order to protect a certain asset, it is useful to be able to assure that the set of intercept orbits does not contain a hostile threat. There are a variety of other ways to pose this problem, but the common theme is constantly searching a large set of orbits to find previously unknown objects.

The second type of search is to perform follow up on an object where its location is not entirely known. A prime example of this is the follow up on an object with a prior characterized by an admissible region. This can be broadened to searching for debris after a break up event, to search for an object that has maneuvered, and reacquisition of an catalog object with sufficiently large uncertainties. If the search region for this object is large, the search strategies may be similar to that of the custody problem, while for a small search region it becomes more feasible.

Methodology

The first requirement is an analytic formulation of the problem. An EOS tasking scheme will be thought of as a series of observations taken at a series of fixed angular coordinates. These discrete task locations can consist of any number of observations taken at any locations in any order. Quantities like exposure time and number of observations taken at each location could be varied, as well as characteristics of the sensor, though this particular work fixes these quantities for simplicity. This paper will assume for simplicity that if a sensor looks in the direction of an object, the object is detected. In other words, missed detections are not considered. As this work matures, a

believe and plausibility filter will be incorporated into the search algorithm to better quantify missed detections and false detections.

An analysis on divergence of a search region is presented. By integrating over the divergence of the velocity vector field, the rate of change of the area of a region can be calculated. A region of high divergence will grow quickly, increasing the total number of observations needed to observe it. The implication is, a time optimal algorithm will prioritize high divergence. The goal of this analysis is to provide physical insight into search region divergence and to develop a way exploit instantaneous divergence to develop better search.

An optimization cost function is then proposed as a way to choose a trajectory. This work will look to minimize the amount of time spent searching for the object, while attempting to scan the entire search area defined by prior information. Due to the high dimensional and non-convex search space, this optimization can be difficult to successfully implement. A second cost function which looks at maximizing the divergence at a given time step is also proposed. This cost function is suited for a finite time horizon control approach.

The specific optimization algorithm is a variation on simulated annealing [11]. Because the number of necessary observations determines the size of the state space that must be searched, for long trajectories this optimization becomes infeasible. Instead, the algorithm optimizes each observation along the trajectory in a cycle. The number of observations is preset for this work, as no effective way of varying this number has been found.

In order to test the optimization algorithm, and illustrate its performance behavior to the reader, a series of increasingly complex tests are presented. First, a simple scan of a section of sky is considered. This test case illustrates algorithm convergence and performance, without including performance issues due to a difficult design space. Second, a full handoff scenario is presented. This test case illustrates the difficulty of the tasking problem and the optimization performance on a large, multi-modal, dynamic design space. This test case is also used to present results on the divergence calculation.

A series of simulations are presented, primarily to explore the feasibility of different handoff configurations. The primary independent factors being examined are uncertainty of initial detection, number of follow-up sensors, and geometry of both the sensors and SO. In particular, the geometry of sensors encompasses a large region of varying orbits and relative geometry which is hard to quantify but extremely important to handoff performance and feasibility.

THEORY

Notation and Background

Consider a search region, $\mathcal{S}(t) \subset \mathbb{R}^6$. For this paper, the search region elements are assumed to be orbits consisting of position and velocity at a given time, $\mathbf{x}(t) = [\mathbf{r}^T(t), \mathbf{v}^T(t)]^T \in \mathbb{R}^6$. This search region could be defined in a variety of ways, including from an admissible region, by defining a region of state space to protect, etc. Note that this region is time varying, according to orbital mechanics; the time notation will be dropped unless explicitly necessary.

This paper requires representing orbits within the field of regard of a sensor. An orbit, $\mathbf{x}$, can be

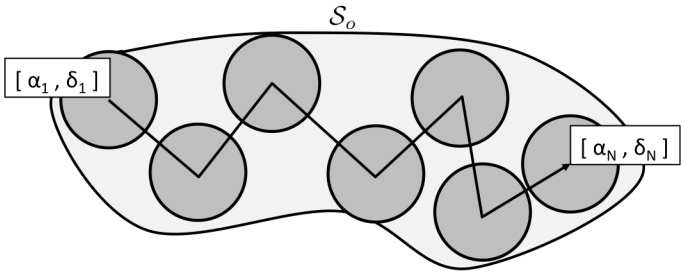

Figure 1. Example of a tasking trajectory over a portion of the sky

partitioned into three sub-components, based on notation used in [16],

$$\mathbf{x} = [\mathbf{x_d}^T, \dot{\mathbf{x}}_\mathbf{d}^T, \mathbf{x_u}^T]^T \tag{1}$$

$$\mathbf{x}_d = [\alpha, \delta]^T \tag{2}$$

$$\dot{\mathbf{x}}_d = [\dot{\alpha}, \dot{\delta}]^T \tag{3}$$

$$\mathbf{x}_u = [\rho, \dot{\rho}]^T. \tag{4}$$

This notation for an optical observer distinguishes between the components instantaneously observed, $\mathbf{x_d}$, the components observed through multiple measurements, $\dot{\mathbf{x}}_\mathbf{d}$, and the components which are unobservable, $\mathbf{x_u}$. This notation can be generalized to any sensor type.

To find a time optimal tasking scheme, a mathematical model must be developed for the system. A sensor is tasked to observe multiple points in the sky, at different time steps, represented by $\mathbf{u}(k) = [\alpha(k), \delta(k)] \in \mathbf{S}(2)$. Note that $\mathbf{S}(2)$ is the unit sphere and is the space in which all angle pairs exist. Because of the many factors that contribute to when an observation takes place, time steps are not necessarily equally spaced, but at arbitrary but known times. The full observation campaign is represented as a pair of vectors of pointing angles,

$$\mathbf{U} = [\boldsymbol{\alpha}, \boldsymbol{\delta}] \tag{5}$$

where the entire campaign consists of N observations. This is illustrated in Figure 1. An EOS makes a detection (or does not) by taking a series of images in a certain location in the sky. The time spent attempting a detection at time step k, will be represented by $t_I(k)$. Once these series of images have been taken, the EOS slews to a new location. Because every sensor mount is different, an arbitrary function, $f_t(\alpha(k), \delta(k), \alpha(k+1), \delta(k+1))$, represents the time it takes a particular sensor to slew from location 1 to location 2.

A requirement for successful search is that every part of $\mathcal{S}(t)$ is observed, requiring a full coverage constraint. Each observation is taken at a location and time in the sky, $\mathbf{u}(k)$, which observes a conical region of state space, $\mathcal{O}(u)$. At each time step, a section of the search space is observed, giving

$$\mathcal{S}(t(k+)) = \mathcal{S}(t(k-)) \setminus \mathcal{O}(u(k)) \tag{6}$$

where k is the time step. This casts the full observation requirement as attempting to reduce the search space $\mathcal{S}$ to the null set. It should be noted that this constraint can be analytically incorporated into admissible region theory. An admissible region is an intersection of a series of sets, each defined

in terms of a constraint,

$$\mathcal{AR} = \bigcap \mathcal{AR}_j \tag{7}$$

$$\mathcal{AR}_j = \{\mathbf{x}_u \in \mathbb{R}^u : g_i(\mathbf{x}_u; \mathbf{x}_d, \dot{\mathbf{x}_d}, \mathbf{k}) \leq 0\} \tag{8}$$

where g_i is a constraint and $\mathbf{k}$ is a parameter vector. When a particular region is observed an no detection is made, it can be assumed that a particular region does not contain the object. This defines a new admissible region,

$$\mathcal{AR}_j = \{\mathbf{x}_u \in \mathbb{R}^u : \phi(\mathbf{x}_u; \mathbf{x}_d, \dot{\mathbf{x}_d}, t_o, t) \notin \mathcal{O}(u)\} \tag{9}$$

which in essence removes whatever section(s) of an admissible region that intersect a particular observation.

Search Area Divergence

What this section looks to determine is both the growth rate of a search region as seen by a particular sensor, and the local regions of expansion and contraction. This section will focus on calculation while the following section will focus on how these calculations can be used to analyze a search region. Assume that an observer, located at $\mathbf{o}(t_o)$, wants to take an observation in this search space at time t_o. First, the search space must be propagated to the appropriate time, via the flow function,

$$\mathcal{S}(t_o) = \boldsymbol{\phi}(\mathcal{S}(t); t_o, t) \tag{10}$$

which is calculated by integrating orbital mechanics. Next, the search space must be propagated into the field of regard of a sensor, through some measurement function $\mathbf{h}$,

$$[\mathbf{x_d}^T, \dot{\mathbf{x_d}}^T]^T = \mathbf{h}(\mathbf{x}) \tag{11}$$

$$\mathcal{S}_o = \{[\mathbf{x_d}^T, \dot{\mathbf{x_d}}^T] : [\mathbf{x_d}^T, \dot{\mathbf{x_d}}^T] = \mathbf{h}(\mathbf{x}), \mathbf{x} \in \mathcal{S}\}. \tag{12}$$

The function $\mathbf{h}$ maps to $[\mathbf{x_d}^T, \dot{\mathbf{x_d}}^T]^T$, the components an observer can measure, while the notation $\mathbf{h}_\alpha$ will be used to represent the the component of $\mathbf{h}$ which calculates just α.

In order efficiently search an area, it would be useful to quantify the expansion of a particular point or region of the sky. The expansion is mathematically captured by the divergence of the angular rate, $\dot{\mathbf{x_d}}$, with respect to angular position, $\mathbf{x_d}$. For an optical sensor, this is more simply,

$$\text{Div} = \nabla_{\mathbf{x_d}} \cdot \dot{\mathbf{x_d}} = \frac{\mathrm{d}\dot{\alpha}}{\mathrm{d}\alpha} + \frac{\mathrm{d}\dot{\delta}}{\mathrm{d}\delta}. \tag{13}$$

Figure 2 shows the divergence changing over a region.

There are two primary concerns with this calculation. First, because an arbitrary search region is being projected into a subspace, multiple orbits, with multiple velocities could all project to a single $\mathbf{x_d}$. This gives a vector field with multiple, and possibly infinite, values at each point. Second, even if the vector field is defined, these derivatives are being calculate based on a set of orbits defined at a previous time, which requires a state transition matrix for every point.

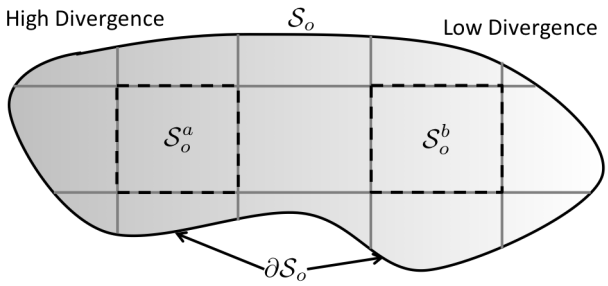

Figure 2. Vector field of $\dot{\alpha}$ and $\dot{\delta}$ as they vary with α and δ

For expansion of a search region as a whole, these problems can be side stepped using Green's Theorem. To review, Green's theorem states that for functions A and B defined over a region $\mathcal{S}_o$, with boundary $\partial\mathcal{S}_o$,

$$\oint_{\partial\mathcal{S}_o}(A\mathrm{d}x + B\mathrm{d}y) = \int\int_{\mathcal{S}_o}\frac{\partial A}{\partial x} - \frac{\partial B}{\partial y}\mathrm{d}x\mathrm{d}y. \tag{14}$$

By setting $A = \dot{\alpha}$, $B = -\dot{\delta}$, $x = \alpha$, and $y = \delta$, this integral implies that the total divergence over the an area is equal to the line integral over the boundary of the orthogonal component of the vector field.

For measuring local areas of divergence within a search region, the Green's Theorem approach provides some insight. In many scenarios, an entire search region may move through the field of regard with some mean velocity, $\dot{\mathbf{x}}_{\mathbf{d}}$. This mean velocity will act uniformally on a line integral and will therefore integrate to zero. By calculating the orthogonal component of $\dot{\mathbf{x}}_{\mathbf{d}} - \dot{\mathbf{x}}_{\mathbf{d}}$ along the boundary, $\partial\mathcal{S}_o$, the local growth or recession of the boundary can be approximated.

When considering a prior set defined by two dimensional manifold, further analysis is possible. An admissible region formed from optical observations is an example of a useful two dimensional manifold of orbits. Such a manifold can be projected though $\mathbf{h}$ into the field of regard and form a reasonable vectorfield. Due to manifold folding, finitely many orbits could project to a single $\mathbf{x}_\mathbf{d}$, but with differing values for $\dot{\mathbf{x}}_\mathbf{d}$. First consider the case such that no folding has occurred and each $\mathbf{x}_\mathbf{d}$ has a single $\dot{\mathbf{x}}_\mathbf{d}$. The search space $\mathcal{S}_o$ can be arbitrarily partitioned into m sub regions,

$$\mathcal{S}_o = \bigcup^m \mathcal{S}_o^i \tag{15}$$

$$\emptyset = \mathcal{S}_o^a \cap \mathcal{S}_o^b \;\forall\; a \neq b \tag{16}$$

where $\mathcal{S}_o^i$ are the non-overlapping partitions. The integral over divergence can be calculated for each partition using Green's theorem. This allows an analytic calculation of local areas of expansion or contraction over the manifold.

If folding occurs, finitely many vector fields, say n, may be defined over a partition, $\mathcal{S}_o^i$. Calculating divergence becomes difficult as there are multiple values for divergence at any given point. This paper proposes defining an upper bound to the divergence based on maximum possible line integral

from a combination of vector fields. Given a series of vector fields, $\dot{\mathbf{x}_\mathbf{d}}^j$ defined over $\mathbf{x_d}$,

$$\oint_{\partial\mathcal{S}_o}(\dot{\alpha}^j \mathrm{d}\alpha + \dot{\delta}^j \mathrm{d}\delta) = \oint_{\partial\mathcal{S}_o} \dot{\mathbf{x}_\mathbf{d}}^{jT} \mathrm{d}\mathbf{x_d}$$
$$\leq \oint_{\partial\mathcal{S}_o} \max_{j\in[1,n]} \left(\dot{\mathbf{x}_\mathbf{d}}^{jT} \mathrm{d}\mathbf{x_d}\right) \tag{17}$$

where the maximum chooses the vector field with the largest outward orthogonal component at any given point. This integral will be larger than any other piece-wise combination of vector fields and will therefore err on the side of caution. This same method can be used for an infinite continuum of orbits, by replacing the maximum with a supremum. As of now, this supremum is only calculable through brute force methods. Further analysis of this supremum will be explored in a future paper.

The last question is this section explores is the determination of the boundary. Because the vector field of $\mathbf{x_d}$ must be defined on this boundary, the orbits associated with the boundary are needed as well. This region which will be denoted by $\partial\mathcal{S}$ is defined as

$$\partial\mathcal{S} = \{\mathbf{x} \in \mathcal{S}(t_o) : \mathbf{h}(\mathbf{x}) \in \partial\mathcal{S}_o\} \tag{18}$$
$$= \mathbf{h}^{-1}(\partial\mathcal{S}_o). \tag{19}$$

Note that $\partial\mathcal{S}$ is an abuse of notation as it is not the boundary of the region $\mathcal{S}_o$ and may not even lie along the boundary. If no folding occurs for a 2 dimensional manifold, the original boundary of the manifold will be associated with the projected boundary.

Exploitation of Divergence

This section focuses on how to use divergence to analyze different search regions. The divergence integral represents the instantaneous rate of change of the area of a region,

$$2\frac{\mathrm{d}}{\mathrm{d}t}|\mathcal{S}_o| = \frac{\mathrm{d}}{\mathrm{d}t}\int\int_{\mathcal{S}_o} 2\mathrm{d}\alpha\mathrm{d}\delta$$
$$= \frac{\mathrm{d}}{\mathrm{d}t}\int\int_{\mathcal{S}_o} \frac{\partial}{\partial\alpha}\alpha + \frac{\partial}{\partial\delta}\delta \ \mathrm{d}\alpha\mathrm{d}\delta$$
$$= \int\int_{\mathcal{S}_o} \frac{\partial}{\partial\alpha}\dot{\alpha} + \frac{\partial}{\partial\delta}\dot{\delta} \ \mathrm{d}\alpha\mathrm{d}\delta. \tag{20}$$

where $|\cdot|$ is a measure of the area of a region, measured in steradians. Given a particular sensor, $\mathbf{o}$, over every integration, t_I, an known area of the sky can be observed, $\mathcal{O}_o(\mathbf{u}(k))$. Then the total change in search region area can be calculated at each time step as,

$$|\mathcal{S}_o(t(k))| \approx |\mathcal{S}_o(t(k-1))| + \frac{\mathrm{d}}{\mathrm{d}t}|\mathcal{S}_o(t(k-1))|(t(k)-t(k-1)) - |\mathcal{S}_o(t(k)) \cap \mathcal{O}_o(\mathbf{u}(k))|. \tag{21}$$

which can easily be show through a Taylor series expansion, ignoring higher order terms. Note that this equation is explicitly dependent on the proposed search trajectory, or control input, $\mathbf{U}$. If $\mathbf{U}$ is totally ineffective, $|\mathcal{S}_o(t(k+1)) \cap \mathcal{O}_o(\mathbf{u}(k+1))| = 0$ for all k, and the resulting area growth by $t(k)$ would be

$$|\mathcal{S}_o(t(k))| \approx |\mathcal{S}_o(t(0))| + \frac{\mathrm{d}}{\mathrm{d}t}|\mathcal{S}_o(t(0))|(t(k)-t(0)). \tag{22}$$

In order to fully observe the search region, the requirement is then

$$|\mathcal{S}_o(t(0))| + \frac{\mathrm{d}}{\mathrm{d}t}|\mathcal{S}_o(t(0))|(t(k) - t(0)) \leq \sum_{k=1}^{N} |\mathcal{S}_o(t(k)) \cap \mathcal{O}_o(\mathbf{u}(k))| \tag{23}$$

A simpler way to see this is, if in general $|\mathcal{S}_o(t(k))| \geq |\mathcal{S}_o(t(k-1))|$, the search problem does not close, while if $|\mathcal{S}_o(t(k))| < |\mathcal{S}_o(t(k-1))|$ the problem closes. This provides a simple and efficient calculation for evaluating whether a search region is searchable. Furthermore, the amount the area changes each time step provides insight into approximately how long a search should take. This analysis is predicated on what is effectively a linearization on the expansion rate of the search region; if $\frac{\mathrm{d}}{\mathrm{d}t}|\mathcal{S}_o(t)|$ is not approximately constant over the interval $t(0)$ to $t(k)$, then Equation (22) does not hold. Orbit dynamics are non-linear are therefore the true solution can diverge from this approximation. This approximation will provide more utility for high altitude orbits such as the geostationary regime.

The partition divergence calculation gives a tool for defining short term high priority search areas. Over a lower divergence region, a region of higher divergence, given equal time, will expand into a larger, harder to search area. For example, in Figure 2, the region of high divergence on the left should be prioritized over the region of low divergence on the right.

It should be noted that the divergence method is probability distribution function (PDF) agnostic. When operating a pure set or a PDF whose effective boundaries are used to define a set, the method gives the same result. This is particularly relevant to admissible region theory, where a set is used to define a PDF. Divergence methods will operate identically on either representation of the admissible region, avoiding analytic confusion.

Search regions can become sufficiently large that a region extends out of the field of regard on an EOS. This may even extend to a ring of orbits around earth, or all of $\mathbf{S}(2)$. In these cases, the total region divergence may no longer be a useful measure, but divergence of partitions is very much still a useful measure. Furthermore, these test cases often encounter the singularity in α and δ at the pole. The divergence integral is still defined and calculable, but care needs to be taken to take into account the non linearity of the space. The best way to handle this involves rotating the definition of $\alpha = 0$ and $\delta = 0$ so that the linearization is centered in whichever partition is being considered.

Time Optimal Cost Function

Typically, a search region has positive over all divergence, though there can exist cases where this may not be the case. Regardless, it can be easily checked for a given search region. Time optimal search is built on the assumption that sensor time is a valuable commodity, and the best way to optimally use a sensor is to spend as little time accomplishing a task as possible. The cost function is then the total time spent over the observation campaign,

$$f_{time}(\boldsymbol{\alpha}, \boldsymbol{\delta}) = \sum_{k=1}^{N-1} [t_{I,k} + f_t(\alpha(k), \delta(k), \alpha(k+1), \delta(k+1))] + t_{I,N} \tag{24}$$

The constraint is difficult to enforce directly as it depends upon the intersection of time varying sets. Instead it can be enforced as a penalty function

$$f_{cost}(\boldsymbol{\alpha}, \boldsymbol{\delta}) = f_{time}(\boldsymbol{\alpha}, \boldsymbol{\delta}) + f_{penalty}(\boldsymbol{\alpha}, \boldsymbol{\delta}; \mathcal{S}) \tag{25}$$

Specifically, this is an exterior penalty function [15]; as the tasking scheme becomes inadmissible, a large cost is added to the function forcing the constraint to be enforced. Penalty functions have a known problem in that they can lead to inadmissible solutions to the optimization. The penalty function in practice is enforced with a discrete point wise approximation of the search space, $\mathcal{S}(t)$, to approximate the percentage of the set contained in the observation,

$$f_{penalty}(\alpha, \delta; \mathcal{S}) = c\,|\mathcal{S}(t(N))| \tag{26}$$

keeping in mind that the search set is reduced in size at every time step, according to Equation (6). The exterior penalty function includes a scaling parameter, c, which is typically increased as iterations of the optimization progress, to better assure the constraint is enforced.

Divergence Greedy Cost Function

Because of the computational difficulty of doing a full optimization a second optimization method is being proposed. This method is again based on the idea that search should be done quickly to make best use of a sensor. Furthermore, it is assumed that there is no PDF to define the location of an object, only a set. This is particularly relevant to follow up on an admissible region. Consider Equation (21). At a given time step, k, the best control is the one which minimizes $\mathcal{S}_o(t)$ for all time. This implies that the observed space should be as big as possible, but it also implies the divergence is as big as possible. By maximizing the divergence in the observed space, the rate of change of area at future time steps is minimized. This optimization can be solved at each time step, but is better posed in a finite time horizon manner. Again, assume a series of observations defined in Equation (5), but assume further that the total number of observations, N defines a finite horizon over which the optimizer will search. A cost function which looks to search the largest area possible with the largest divergence possible would then be

$$f_{Div} = -\sum_{k=1}^{N} \frac{\mathrm{d}}{\mathrm{d}t} |\mathcal{O}_o(\mathbf{u}(k)) \cap \mathcal{S}_o(t(k))| \tag{27}$$

keeping in mind that $\mathcal{S}_o(k)$ changes each time step based on both dynamics and sections being removed by previous observations. Note that the total divergence is proportional to the area which is integrated over, so this cost function will prefer large, highly divergent regions.

SIMULATION TEST RESULTS

Test Problem Results

The first basic problem that will be explored will be divorced from the dynamics of the handoff problem. Because the full time optimization is highly complex, it first tested on a simple problem. The problem on which the optimization will be tested first is coverage of a stationary area of the sky above a particular sensor. This could be thought of as a scan of an area for search and initial detection. The field of view of the sensor is 2 degrees and the space being searched is 4 degrees by 16 degrees. The results of this test can be seen in Figure 3.

The difficulty of the traveling salesman problem, implies that a true optimum is difficult to find. Keep in mind that the final goal of this optimization is to operate on trajectories with hundreds of observation. Because the optimization technique is highly stochastic, the final path is not repeatable. While stochasticity makes final solutions unpredictable, but is needed to avoid the plethora of local minima. Even with these caveats, the final trajectory finds good coverage.

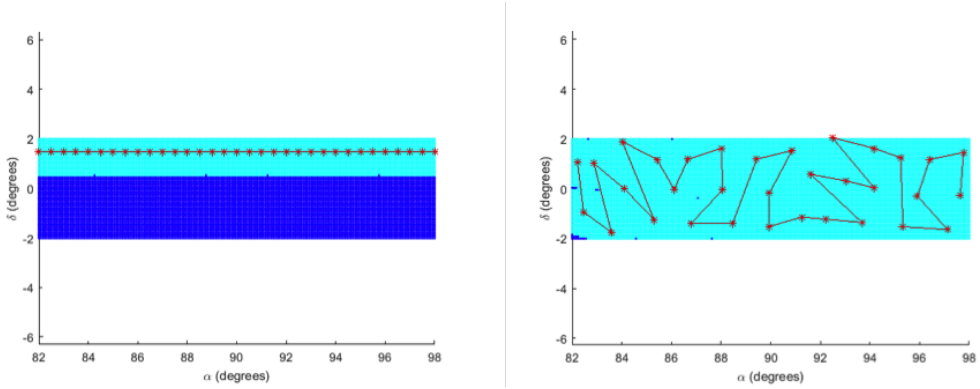

(a) (b)

Figure 3. Trajectory before and after proposed optimization algorithm

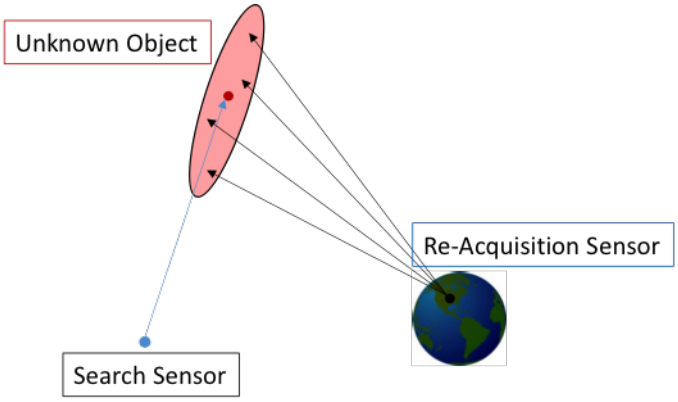

Figure 4. Geometry of first and second observers

Implementation Details

An initial detection is made by a space based sensor intended for search alone, as seen in Figure 4. The detection is determined to be high priority and follow-up is therefore needed. The detection consists of a series of unit vectors over a short period of time.

The initial short arc observation is used to create an admissible region. The admissible region is sampled by first generating random measurements from the uncertainties. For each sampled measurement, a respective admissible region is sampled to complete the particle. This is the uncertain formulation of an admissible region [16]. The admissible region is constrained with maximum energy, minimum radius of periapsis, maximum inclination of 90 degrees, and maximum eccentricity of 0.9.

In practice, the initial guess given to the optimization algorithm is extremely important. Local optima are dense, and it can be difficult for a search algorithm to make dramatic changes from initial conditions. Initial guesses have been set to intuitively good trajectories to begin with (such as a bisecting path) and lead to similar, but more optimal final trajectory (such as a zig zagging path). A variety of initial paths should be tried to fully explore the state space. This is a common procedure in simulated annealing; while the stochastic algorithm provides some design space exploration,

multiple runs are needed with different initial conditions to allow acceptable exploration. Another observation from the variety of initial trajectories tried is that locations of high particle divergence should be searched before areas of low divergence. Areas of high divergence will take more observations to achieve full coverage, the longer an observer waits to take observations. Conversely, low divergence implies a lenience to delayed observations. This can be included in the initial trajectory to manually explore a part of the design space known to contain a good minimum.

The primary optimization technique used is simulated annealing. Because many of the trajectories consist of a large number of observations which all must be simultaneously optimized, each point along the trajectory is optimized individually. A loop cycles through each point along the trajectory, and a single iteration of simulated annealing is run on the point. This entire process is then run multiple times.

Space to Ground Handoff Test

A group of ground based observers are located at Maui, [20.80^o N, 156.33^o W], $\mathbf{o}_2$, while a space based observer, $\mathbf{o}_1$, is located in the 160^o W geostationary orbit slot. An unknown space object, $\mathbf{x}_{RSO}$, located in the 130^o W geostationary orbit slot, is first detected by the space based observer. The space based observer takes 5 measurements, each 1 second apart with Gaussian distributive noise with 1 arc second standard deviation. Two ground based observers are tasked with reacquiring the object based on the information in the measurements taken by the space based observers. Follow up sensors have a one degree by one degree field of view, and take $t_I = 10$ seconds to collect data in a certain area of the sky. The follow up observers are not allowed to attempt follow up until 1 hour has passed.

First, the observations from $\mathbf{o}_1$ need to be quantified as a set of possible orbits. This is done through admissible region theory, using a discrete point wise approximation, using 10,000 particles. Because there will be significant uncertainty in the measurement used for the admissible region, an uncertain admissible region is used [16]. The uncertain admissible region is generated by sampling particles from the measurement uncertainties, and sampling a single point from the respective admissible regions. The random samples from the admissible region are propagated over a sufficient time period to encompass the entire observation campaign, and results are saved at one second intervals. The cost function, when checking the observed particles of each observation, uses the propagated particles from the most recent iteration.

This particular test uses two collocated sensors for follow-up. The initial trajectory has both sensors observing at opposite ends of the search space and slewing toward the center. A preset number of 120 observations is set based on the approximate size of the search space.

Results from the optimization are shown in the Figure 5. As time progresses, the particles (and therefore search space) grows. The total observation time is around 10 minutes.

Divergence Analysis of Search Region

The observers in this example have a one degree by one degree field of view, which is equal to approximately $|\mathcal{O}_o| = 3.0 \times 10^{-4}$ sr, while the integration time is 10 s. The total area of the region is $|\mathcal{S}_o(0)| = 0.033$ sr, while the area rate of change, calculated using Green's Theorem, is $\frac{\mathrm{d}}{\mathrm{d}t}|\mathcal{S}_o(0)| = 6.0^{-6}$ sr per second. Over each time step

$$|\mathcal{S}_o(t(k))| \approx |\mathcal{S}_o(t(k-1))| + 6.0^{-6}\frac{\mathrm{sr}}{\mathrm{s}} \times 10\mathrm{s} - 2 \times 3.0 \times 10^{-4}\mathrm{sr} \tag{28}$$

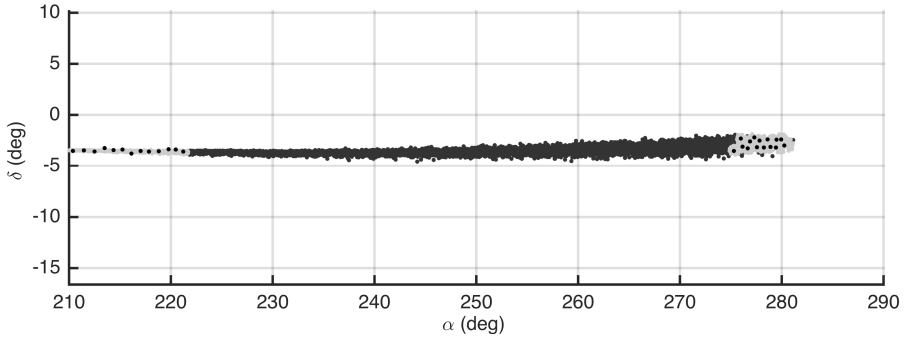

(a) Trajectory after 150 seconds

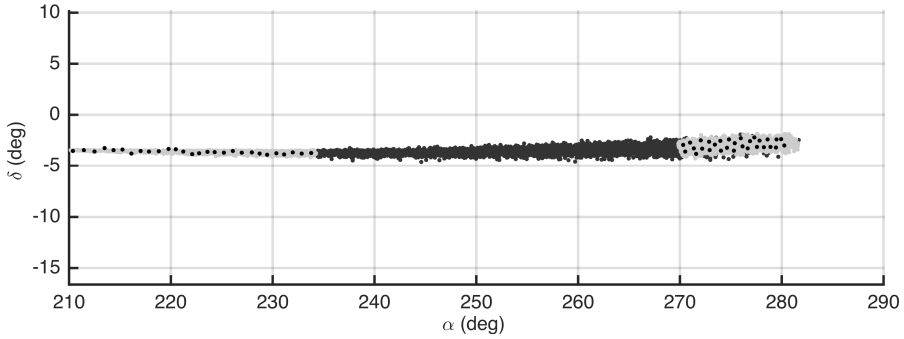

(b) Trajectory after 300 seconds

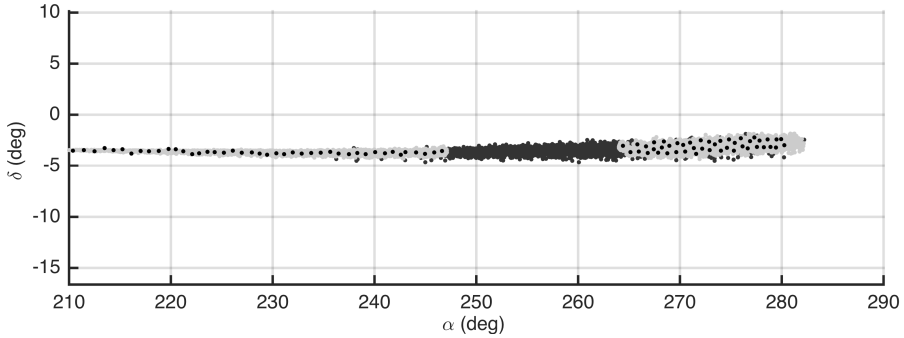

(c) Trajectory after 450 seconds

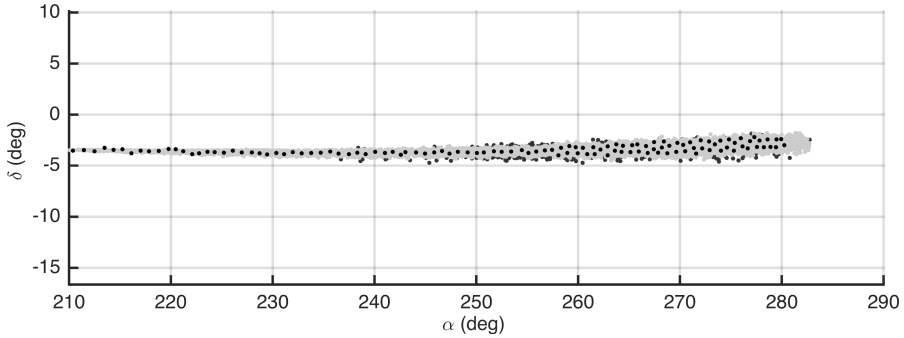

(d) Trajectory after 600 seconds

Figure 5. Trajectory on expanding search space over time

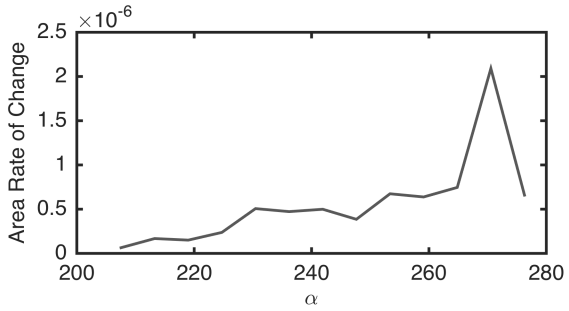

Figure 6. Local divergence of search region

Table 1. Table of results included

	Offset	inclination	Results Shown
Table 3	30^o	0^o	Percent coverage, expected campaign length
Table 2	60^o	0^o	Percent coverage, expected campaign length
Table 4	10^o	0^o	Follow-up time for 95% coverage
Table 5	10^o	3^o	Follow-up time for 95% coverage
Table 6	10^o	7^o	Follow-up time for 95% coverage

Given the initial area of 0.033 sr, it should take approximately 60 timesteps to fully observe the region. The local regions of divergence are also analyzed across the search region. These local areas of divergence are plotted as a function of right ascension in Figure 6.

RESULTS FOR DIFFERENT SPACE BASED SENSOR HANDOFF SCENARIOS

A primary motivation of this work is to explore different space based sensor scenarios. A variety of simulations have been run to explore when follow-up is feasible or infeasible, and what type of follow-up times can be expected. This section presents several tables exploring follow up time and percent coverage. The results are shown over variable handoff times and tracklet lengths. The handoff time is the time between the first measurement in the initial tracklet and the first observation in the follow-up trajectory. The initial detection tracklet is a series of angles-only measurements 1 second apart, with 1 arc second standard deviation Gaussian noise. The tracklets are used to estimate the angular rates, with appropriate uncertainties.

This section presents results of both the percent coverage and expected number of follow up observations. In all cases the first observer is in the 160^o W GEO slot geostationary orbit and the second follow-up observer is located on Maui, [20.80^o N, 156.33^o W]. The unknown space object is in a geostationary orbit, but the exact slot and inclination is altered between test cases, in order to explore the effect of geometry. The offset of the unknown object is measured in degrees east of the 160 W GEO slot. For inclined orbits, the unknown object is assumed to be at the ascending node of its orbit. Table 1 details the results included in this section.

Varying Range

The first set of results looks at the percent coverage achieved by two 1×1 degree field of view sensors over a 300 observation campaign. The campaign takes around 25 minutes for all test cases. 300 observations may be more or less observations than needed, but using the same number for

Table 2. Two observers, 300 observations, GEO to GEO, 60 degrees offset

		Number of observations in initial detection tracklet				
		3 Obs	5 Obs	7 Obs	9 Obs	11 Obs
Handoff Time	60 min	89% , 244	98.5%, 90	100% , 54	100% , 40	100%, 33
	90 min	72.5%, 458	93.5%, 155	98% , 96	98.5%, 74	99% , 62
	120 min	63% , 1176	81.5%, 267	91% , 157	92% , 125	94% , 110
	150 min	21.5%, N/A	57.5%, 601	55.5%, 317	53.5%, 228	53% , 208
	180 min	15% , N/A	35.5%, N/A	38% , N/A	34% , 1287	34% , 239

Table 3. Two observers, 300 observations, GEO to GEO, 30 degree offset

		Number of observations in initial detection tracklet				
		3 Obs	5 Obs	7 Obs	9 Obs	11 Obs
Handoff Time	60 min	97% , 143	99.5%, 54	99% , 34	99% , 25	99.5%, 20
	90 min	90.5%, 256	99.5%, 96	99.5%, 59	99.5%, 45	99.5%, 38
	120 min	80.5%, 470	95.5%, 151	98% , 98	99% , 77	99% , 67
	150 min	61% , 1680	84.2%, 262	86.5%, 172	91% , 133	93.5%, 117
	180 min	39.5%, N/A	38.5%, N/A	49.5%, 559	53.5%, 337	56.5%, 268

every case makes the results more comparable. The optimization was run for a fixed number of iterations with the same parameters for every case (the stochastic optimization typically means true convergence never occurs). The first set of results are displayed in terms of percent coverage, which is calculated as the percentage of particles observed by the final trajectory. The second set of results are displayed in terms of minimum number of observations, as calculated via Equation (23). Results should be treated as initial findings, as with a better optimization method with variable numbers of observations should perform better in certain test cases.

Tables 2 and 3 all look at a two-observer follow-up with an offset of 60 and 30 degrees. These tables are an examination of what is possible given a certain number of sensors and certain amount of time. As one would expect, feasibility improves with lower initial uncertainty and shorter handoff times. Results showing 95% coverage or more imply that full coverage is possible, while results under 50% coverage are typically indicative of a search space diverging faster than a sensor can search. These results align with the predicted campaign length; the linearization used in Equations (23) is not reliable after the 300 observation campaign. An interesting result of this analysis is, assuming the short arc assumption holds, more observations in the initial tracklet give diminishing gains after a certain point.

Varying Inclination

The second set of results looks at the total time necessary to achieve 95% coverage of the search space. These results again use two follow-up observers, both with a 1×1 degrees field of view. The offset is set at 10^o for this entire section. These results primarily look at the effect of inclination on total campaign length. Specifically, the inclination of the unknown space object is varied while keeping the initial position fixed. The results shown in Tables 4, 5, and 6 correspond to zero, three, and seven degrees inclination.

Table 4. Time for follow-up, two observers, GEO to GEO, 10 degrees difference, 0 degrees inclination

		Number of observations in initial detection tracklet				
		3 Obs	5 Obs	7 Obs	9 Obs	11 Obs
Handoff Time	30 min	7 min	5 min	5 min	5 min	5 min
	60 min	16 min	6.5 min	6 min	6 min	6 min
	90 min		14 min	7.5 min	7 min	6 min
	120 min			16 min	12 min	10 min

Table 5. Time For follow-up, two observers, GEO to GEO, 10 degree difference, 3 degrees inclination

		Number of observations in initial detection tracklet				
		3 Obs	5 Obs	7 Obs	9 Obs	11 Obs
Handoff Time	30 min	7.5 min	5 min	5 min	5 min	5 min
	60 min	17 min	7 min	5.5 min	5 min	6 min
	90 min	$>$17 min	11 min	7 min	6 min	6 min
	120 min					$>$17 min

Table 6. Time for follow-up, two observers, GEO to GEO, 10 degree difference, 7 degree inclination

		Number of observations in initial detection tracklet				
		3 Obs	5 Obs	7 Obs	9 Obs	11 Obs
Handoff Time	30 min	8 min	6 min	6 min	6 min	6 min
	60 min	$\sim$	9 min	7.5 min	7 min	7 min
	90 min					$\sim$

CONCLUSION

Intuitive Concepts and Conclusions

The first major result the paper shows is geometry is key in enabling feasibility of handoff and follow-up. In particular the key is to avoid hypothesis orbits at low altitudes. Typically, hypothesis orbits at high altitudes have low accelerations and therefore diverge slowly, while low altitudes almost always have high accelerations and diverge quickly. This is why all examples use a GEO observer and GEO target, as the line of site creates only orbits at high altitude. Inclination also leads to high divergence. More specifically, if the initial observer and target are out of plane with each other, the hypotheses tend to diverge more quickly. This is because the plane of the orbit is less well understood. These results are intuitive and unsurprising.

Even with perfect knowledge of the initial short arc measurement, and a therefore perfectly known admissible region (no uncertainties), the dynamics of the different admissible orbits will diverge after sufficient time. This implies that taking extra measurements does very little to help reacquisition after sufficiently low uncertainties have been achieved. This also implies that for a given geometry, there exists a handoff time after which reacquisition is fruitless.

Divergence provides a measure of the spread of a set. This tool provides a useful method for analyzing regions of the sky, and further work should be done to tie in divergence with search optimization.

Limitations of Method

As mentioned above, the relative geometry of initial observer and unknown space object is immensely important to follow-up. Because these factors are largely out of the operator's control, this makes mission planning difficult. However region divergence provides an efficient method to predict this.

For LEO based observers, full coverage is practically impossible without instantaneous handoff. Typically, some feasible hypotheses will exist in a range of orbits in LEO all of which will quickly circle the earth while the hypotheses at GEO will stay stationary with respect to the surface of the earth.

Sufficient uncertainty can make re-acquisition impossible, but for reasonable uncertainty levels, this is less of a concern than other factors. A sufficiently long handoff time exists for all cases, past which reacquisition is impossible. In best case scenario, full coverage search can still require extensive search time. There is no way to get around this for many of the scenarios considered, if full coverage is the goal.

Opportunities for Future Work

This section describes results which appear to be possible based on the work presented, but are not included in this paper. Results in certain cases are promising enough to show the utility of space based sensors for domain awareness. Geometries do exist which allow handoff in an efficient manner, and design work can be done to make these geometries more abundant. There is therefore an opportunity to further explore SSA mission concepts using this work.

This work could provide high utility with an ability to define high priority subspaces. Instead of attempting to perform a full space search, sub-regions can be defined based on, for example, conjunction analysis. This may lead to opportunities to obtain search regions which can more

feasibly be searched. Further applications are possible by utilizing new and different ways to define a search space.

ACKNOWLEDGMENT

This research was conducted with Government support under and awarded by DoD, Air Force Office of Scientific Research, National Defense Science and Engineering Graduate (NDSEG) Fellowship, 32 CFR 168a. We would like to acknowledge and thank the Air Force Research Laboratory Scholars Program for supporting this project. I also need to thank my fellow graduate students at Georgia Tech, particularly Andris Jaunzemis and Johnny Worthy. Grad school can not be conquered alone.

REFERENCES

[1] Ossama Omar Abdelkhalik, Daniele Mortari, and John L Junkins. Space surveillance with star trackers. part ii: Orbit estimation. In *Space Flight Mechanics Meeting Conference*, 2006.

[2] Travis Blake. Space domain awareness (sda). Technical report, DTIC Document, 2011.

[3] Kyle J DeMars and Moriba K Jah. Probabilistic initial orbit determination using gaussian mixture models. *Journal of Guidance, Control, and Dynamics*, 36(5):1324–1335, 2013.

[4] Kyle J DeMars, Moriba K Jah, and Paul W Schumacher. Initial orbit determination using short-arc angle and angle rate data. *Aerospace and Electronic Systems, IEEE Transactions on*, 48(3):2628–2637, 2012.

[5] R S Erwin, P Albuquerque, S K Jayaweera, and I Hussein. Dynamic sensor tasking for space situational awareness. In *Proceedings of the 2010 American Control Conference*. Institute of Electrical & Electronics Engineers (IEEE), jun 2010. URL: http://dx.doi.org/10.1109/acc.2010.5530989, doi:10.1109/acc.2010.5530989.

[6] Gregory Gutin and Abraham P. Punnen, editors. *The Traveling Salesman Problem and Its Variations*. Springer US, 2007. URL: http://dx.doi.org/10.1007/b101971, doi:10.1007/b101971.

[7] T Hobson, I Clarkson, Travis Bessell, Mark Rutten, Neil Gordon, Nicholas Moretti, and Brittany Morreale. Catalogue creation for space situational awareness with optical sensors. In *Advanced Maui Optical and Space Surveillance Technologies Conference*, 2016.

[8] T Hobson, N Gordon, I Clarkson, Mark Rutten, and T Bessell. Dynamic steering for improved sensor autonomy and catalogue maintenance. In *Advanced Maui Optical and Space Surveillance Technologies Conference, Wailea, HI*, 2014.

[9] Tyler A. Hobson and I. Vaughan L. Clarkson. A particle-based search strategy for improved space situational awareness. In *2013 Asilomar Conference on Signals, Systems and Computers*. Institute of Electrical & Electronics Engineers (IEEE), nov 2013. URL: http://dx.doi.org/10.1109/acssc.2013.6810418, doi:10.1109/acssc.2013.6810418.

[10] A Jaunzemis, M Holzinger, and M Jah. Evidence-based sensor tasking for space domain awareness. In *Advanced Maui Optical and Space Surveillance Technologies Conference*, 2016.

[11] S. Kirkpatrick, C. D. Gelatt, and M. P. Vecchi. Optimization by simulated annealing. *Science*, 220(4598):671–680, may 1983. URL: http://dx.doi.org/10.1126/science.220.4598.671, doi:10.1126/science.220.4598.671.

[12] Andrea Milani, Giovanni F Gronchi, Mattia de'Michieli Vitturi, and Zoran Knežević. Orbit determination with very short arcs. i admissible regions. *Celestial Mechanics and Dynamical Astronomy*, 90(1-2):57–85, 2004.

[13] Brad Sease, Kevin Schmittle, and Brien Flewelling. Multi-observer resident space object discrimination and ranging. In *AAS/AIAA Space Flight Mechanics Meeting*, 2015.

[14] Z. Sunberg, S. Chakravorty, and R. Erwin. Information space sensor tasking for space situational awareness. In *2014 American Control Conference*. Institute of Electrical and Electronics Engineers (IEEE), jun 2014. URL: http://dx.doi.org/10.1109/acc.2014.6858922, doi:10.1109/acc.2014.6858922.

[15] Garret N. Vanderplaats. Multidiscipline design optimization. *Applied Mechanics Reviews*, 41(6):257, jun 1988. URL: http://dx.doi.org/10.1115/1.3151897, doi:10.1115/1.3151897.

[16] Johnny L Worthy III and Marcus J Holzinger. Incorporating uncertainty in admissible regions for uncorrelated detections. *Journal of Guidance, Control, and Dynamics*, 0(0):1–17, 2015. URL: http://dx.doi.org/10.2514/1.g000890, doi:{10.2514/1.g000890}.

[17] Johnny L Worthy III and Marcus J Holzinger. Use of uninformative priors to initialize state estimation for dynamical systems. In *AIAA/AAS Astrodynamics Specialist Conference*, 2015.

[18] Johnny L Worthy III, Marcus J Holzinger, and Daniel J Scheere. An optimization based approach to corellation of observations with uncertainty. In *AIAA/AAS Space Flight Mechanics Conference*, 2016.